# Sustainable Chitosan Supported Magnetite Nanocomposites for Sequestration of Rhodamine B Dye from the Environment



# Sustainable Chitosan Supported Magnetite Nanocomposites for Sequestration of Rhodamine B Dye from the Environment

**A. O. Dada [1,2,3,4,5*], A. A. Inyinbor [1,2,4], B. E. Tokula [1,2,3,4], C. O. Ajanaku[1], S. Ayo-Akere[1], D. F. Latona [6], K.O. Ajanaku [1]**

[1] Industrial Chemistry Programme, Nanotechnology Laboratory, Department of Physical Sciences, Landmark University, P.M.B.1001, Omu-Aran, Kwara, Nigeria

[2] Landmark University Sustainable Development Goal 6: Clean Water and Sanitation, P.M.B.1001, Omu-Aran, Kwara, Nigeria

[3] Landmark University Sustainable Development Goal 7: Affordable and Clean Energy, P.M.B.1001, Omu-Aran, Kwara, Nigeria

[4] Landmark University Sustainable Development Goal 11: Sustainable Cities and Communities, P.M.B.1001, Omu-Aran, Kwara, Nigeria

[5] Landmark University Sustainable Development Goal 14: Life Below Water, P.M.B.1001, Omu-Aran, Kwara, Nigeria

[6] Department of Pure & Applied Chemistry, Faculty of Basic and Applied Sciences, Osun State University, Osogbo, 210001, Nigeria

**Email and ORCID ID of all Authors**

Email:- dada.oluwasogo@lmu.edu.ng; ORCID: 0000-0001-8645-0691
Email:- inyinbor.adejumoke@lmu.edu.ng; ORCID: 0000-0001-8321-3148
Email:- tokula.blessing@lmu.edu.ng ; ORDCID: 0000-0001-6261-0603
Email:- ajanaku.christiana@lmu.edu.ng ORCID: 0000-0001-6408-2779
Email:- ayoakere.sylvester@lmu.edu.ng
E-mail: dayo.latona@uniosun.edu.ng ORCID: 0000-0002-2722-6734
E-mail: ajanku.kolawale@lmu.edu.ng ; ORCID: 0000-0002-5320-845X

**Corresponding authors email:** dada.oluwasogo@lmu.edu.ng

**Abstract**

This study investigated the sustainable chitosan supported magnetite nanocomposites (C-$Fe_3O_4$) for sequestration of Rhodamine B (RhB) Dye from environment. The synthesis of C-$Fe_3O_4$, its physicochemical characterization and synergistic influence of initial concentration of the dye and time of contact with the adsorbent during the sorption of Rhodamine B (RhB) on C-$Fe_3O_4$ were studied. The physicochemical properties indicated better equilibration via bulk density of 0.731 g/cm$^3$, moisture content 7.2, point of zero charge (PZC) of 4 indicated suitability for RhB. Functional group of C-$Fe_3O_4$ determined by FTIR revealed characteristics peaks at 3433 cm$^{-1}$ and 698 – 478 cm$^{-1}$ confirming the successful formation by incorporation of chitosan and magnetite nanoparticles. Synergistic influence of the time of contact and initial concentration of Rb dye influenced the dye sorption. Effective adsorption of RhB onto C-$Fe_3O_4$ was studied using batch adsorption techniques at initial concentration (200 – 1000 ppm), contact time (10 – 120 min), stirring speed (120 rpm), temperature of 25 $^oC$ and adsorbent dosage of 100 mg. Rapid adsorption of RhB onto C-$Fe_3O_4$ was obtained at 10 min with 96.9% removal efficiency at highest RhB concentration of 1000 ppm. The study revealed the efficacy of contact time and initial dye concentration as imperative operational parameters majorly influencing sorption study.

**Keywords:** Sustainable magnetite nanocomposite; Rhodamine B Dye; Adsorption; Environment; Chemical Removal efficiency

## 1. Introduction

Anthropogenic activities as a result of various industrial development has been reported to aid dye release into the environment [1]. The majority of industries that utilize dyes to provide color to their final goods are textile, leather, paper, plastics, and cosmetics[2]. This has raised concerns on a global scale, because dye is a risk to the environment and may bioaccumulate, which could eventually have an impact on humans and aquatic life through the food chain [3]. Wastewater with even trace amounts of color reduces dissolved oxygen and light penetration, it can have a negative impact on aquatic life. Dye's negative effects have been connected to some mutagenic and carcinogenic effects [4]. The dye being studied in this study is rhodamine B. This cationic dye is widely utilized in the textile sector because of its high solubility and good fastness on materials. But according to reports, it causes cancer [5]. Impact of these dyes have adulterated water and environment quality thereby militating against some of the sustainable development goals (SDG). The actualization of the reality of SDG 13-climate action, SDG 14-life below water and SDG 6-clean water and sanitation and would be vague if the indiscriminately introduced dyes are not addressed.

Chemical precipitation process, ion exchange technique, solvent extraction process, membrane processes, reverse osmosis technique and electro dialysis are some of the techniques at which have been applied for eliminating dyes from wastewater [6]. These techniques are expensive and have several drawbacks, such as the inability to completely remove dyes, the high energy and reagent consumption, and the production of hazardous sludge and other by- products that need to be treated or disposed of [7]. Among the various conventional techniques (Biological, chemical and physical methods) for dye removal, adsorption technique has demonstrated to be unique, cost-efficient, rapid, with greater ease in practicality [8]. Chitosan is among the intriguing organic substances being used for adsorption purposes is chitosan. The presence of $–NH_2$ and –OH groups in its molecular structure is primarily responsible for the likelihood of adsorption surfaces between adsorbate molecules and chitosan molecules[9]. Hence Chitosan has been applied for the sequestration of various emerging contaminants because of its low cost, ease of polymerization and functionalization, and high stability [10].

In recent years, the creation of nano-adsorbents and their uses in environmental remediation are also being investigated by researchers[11]. Nanomaterials have several applications, including optical devices, environmental remediation, medicinal, catalysis, and more, and their use is constantly expanding [12][13]. To the scope of our knowledge, no known reports exist on the application of chitosan supported magnetite nanocomposites for the sorption of Rb dye. This study therefore focuses on the physicochemical characterization and synergistic effect of operational parameters on adsorptive uptake of Rb on chitosan supported magnetite nanocomposites.

## 2. Materials and Methods

### *2.1 Materials Collection*

All chemicals used for this research were of analytical grade and were purchased from Sigma Aldrich and used for this research. Materials and Equipment used include; Iron Chloride hexahydrate (98.2 % purity, CAS-10025-77-1), sodium borohydride (99 % purity, CAS-16940-

66-2), chitosan (CAS-9012-76-4), Isopropyl alcohol (CAS: 67-63-0, 98% purity), Sodium Hydroxide (1310-73-2, 98 % purity), Hydrochloric acid (95% purity), filter paper, measuring cylinders, pH meter (model: Hanna HI98107), Rhodamine B, FTIR Spectrophotometer (model: PerkinElmer), UV-Vis Spectrophotometer (model: UV 6300PC-VWR).

*2.2 Preparation of Magnetite Nanoparticle*

The nanoscale magnetite nanoparticle was prepared using the chemical reduction process reported by Mohammadi et al., [14]. The synthesis is described by the Equation 1:

$$4Fe^{3+} + 3BH^{-}_{4} + 9H_2O \rightarrow 4Fe^{0} \downarrow + 3H_2BO^{-}_{3} + 6H_2 \quad (1)$$

0.023 M $FeCl_3$ was synthesized by adding 6.22 g of $FeCl_3.6H_2O$ into water (distilled) and stirred well. Also 0.123 M $NaBH_4$ solution was prepared i.e. 4.73g of $NaBH_4$ was dissolved in 1000ml de-ionized water, the solutions were then reacted together drop wise using burette and Erlenmeyer flask, 0.123 M $NaBH_4$ as the titrant and 0.023M $FeCl_3$ as titrant while stirring at 200 rpm using magnetic stirrer. The mixture was allowed to stir for 20 mins after adding all the borohydride solution, then left to age for 24 hours, nanoscale particles were then removed from the solution by utilizing vacuum filtration technique alongside a millipore filter paper (0.45µm). The black solid nanoscale particles were washed twice with 25 ml isopropyl alcohol, this washing process is necessary to prevent the oxidation of zero-valent iron nanoscale particles [15].

*2.3 Preparation of chitosan supported magnetite Nanocomposite*

This was done in accordance with a similar process reported by Imran et al.,[3]. Chitosan supported magnetite nanocomposite was prepared with $FeCl_3$ and chitosan in a ratio of 1:1. Firstly, chitosan (4g) was accurately weighed into 2% volume of acetic acid (100 mL). For a period of 4 hours, the obtained mixture was agitated continuously on a magnetic stirrer to obtain a homogenous mixture.

Following that, 10 g of the produced iron nano-composites were added to 100 ml of 4% chitosan and stirred continuously with a magnetic stirrer for 4 hours. To separate the solution, a Millipore filter paper (0.45m) was employed for vacuum filtration, and NaOH (0.1 M) was utilized to neutralize it. After that, the chitosan-supported magnetite nanoparticles were oven dried overnight at 50 degrees Celsius and stored in an airtight container [17].

*2.4 Physicochemical Characterization*

*2.4.1 Bulk Density*

The bulk density was derived via the Archimedes principle. The reported procedure by Dada et al., [18] was followed by measuring accurately an empty cylinders weight and a cylinder containing 5 ml of the adsorbate. Equation 2 was applied for the bulk density determination.

$$\text{B.D} = (w_2 - w_1)/v \quad (2)$$

Where $w_1$ represents the empty measuring cylinder's weight, $w_2$ stands for the weight of cylinder + adsorbate and v represents the cylinder's volume.

### *2.4.2 Moisture Content Determination*

The moisture content value was obtained by heating 1g of the adsorbent and heating in the oven for a period of 5 hours with the aid of a crucible at a temperature of 75 ºC. The weight of the crucible was taken before and after heating to determine the left amount of moisture present in the adsorbent. The moisture content equation is given in the equation 3.

$$\% \text{ moisture content} = \frac{w_2 - w_3}{w_2 - w_1} * 100 \quad (3)$$

Where $W_1$ is the empty dry crucibles weight, $W_2$ is the weight of crucible and 1g of the adsorbent before heating and $w_3$ weight of 1g of adsorbent contained in the crucible after heating [19].

### *2.4.3 pH point of Zero charge ($pH_{pzc}$)*

The technique outlined by Tokula *et al* [20] was used to determine the pH point of zero charge (pHpzc) of the adsorbent.. This was done by bringing 0.1g of the adsorbent into contact with 25ml of 0.1M NaCl, the initial pH of which had been previously changed between pH 2 and 10 using HCl or NaOH. The final pH values were tested 24 hours after which the vessels were wrapped and put on a shaker. Calculated and plotted against the initial pH was the observed difference between the final and initial pHs. The pHpzc was found at the point where the resulting curve and the vertical axis intersected.

### *2.4.4 Analysis Using the Fourier Transform Infrared (FTIR)Spectroscopy.*

The FTIR characterization was carried out with the Shimazu model FTIR. The several functional groups that were present on the exterior of C-$Fe_3O_4$ were identified via the analysis of FTIR. The different bonds and groups of bonds vibrate at distinct frequencies according to FTIR. As a result, samples that were subjected to infrared radiation absorbed the energy at frequencies unique to the molecules in the sample [21].

## *2.5 Adsorption Studies*

The sorption of Rhodamine B to ascertain the adsorption capacity of C-$Fe_3O_4$, de-ionized water was used to dissolve 0.01 M of Rhodamine B, and the mixture was then added to a 1000 mL standard flask to prepare 10 ppm. Serial dilution was done to prepare lower concentration that were used for the adsorption studies. 1, 2, 3, 4, and 5 ppm initial concentrations were used for the work in less than 50 minutes of preparation, so as to ensure that concentration of the adsorbate remain constant prior to sorption studies [22].

### *2.5.1 Influence of Initial RhB Concentration, Time of Contact and Initial concentration.*

The Influence of Contact time, initial concentration and temperature on the adsorption of Rhodamine B was monitored [23][24]. This was done by weighing adsorbent (0.1 g) into a beaker and agitating with various concentrations (1-5 mg/L) of RhB dye.

*2.5.2 Effect of pH*

Different concentrations of Rhodamine B (1-5) mg/L dye were formed by diluting the stock solution using the serial dilution method, it was then agitated with 0.1g of the adsorbents with 25 mL of RhB at various pH ranging from 1-12 to determine the optimum pH for RhB adsorption [22].

*2.5.3 Influence of Contact Time*

Different time durations, (10, 20, 30, 60, 90 and 120) mins were used to establish the equilibrium time. A known concentration of the adsorbate (1, 2, 3, 4 and 5) ppm was agitated with 0.1 g of the adsorbents at room temperature [25].

## 3. Results and Discussion

*3.1 Characterization of Chitosan supported magnetite (Physicochemical)*

The FTIR, moisture content, bulk density, and the pH point of zero charge (pHpzc) were used to analyze the synthesized Chitosan supported magnetite. Table 1 shows results for the moisture content, point of zero charge and bulk density. The point where a surface area possesses a net neutral charge, is said to be at the point of zero charge (pHpzc) [26]. Since C-$Fe_3O_4$ has a pH of 4, it can be used to adsorb the dye at a lower pH than the (pHpzc).

According to Table 1, the bulk density of the chitosan supported iron signifies a suitable equilibration with RhB Dye, thus reducing its floating abilities. The moisture content of chitosan supported iron nanoparticle which is 7.2 signifies a low level of moisture. This indicates that the experimental weight is equilibrium with the weighed amount [27].

Table 1: The physico-Chemical properties of C-$Fe_3O_4$ used for Rhodamine B Dye Uptake

| **Parameters** | **C-$Fe_3O_4$** |
|---|---|
| Bulk Density (g/$cm^3$) | 0.731 |
| Moisture content | 7.2 |
| Point of zero charge ($pH_{pzc}$) | 4 |

*3.2 Fourier Transform Infrared Spectroscopy (FTIR) Spectroscopy Results*

Prior to adsorption, Fig. 1 demonstrated the FTIR spectrum of C-$Fe_3O_4$ revealed the surface functional groups depicting the molecular environments before interaction with Rhodamine B [28].

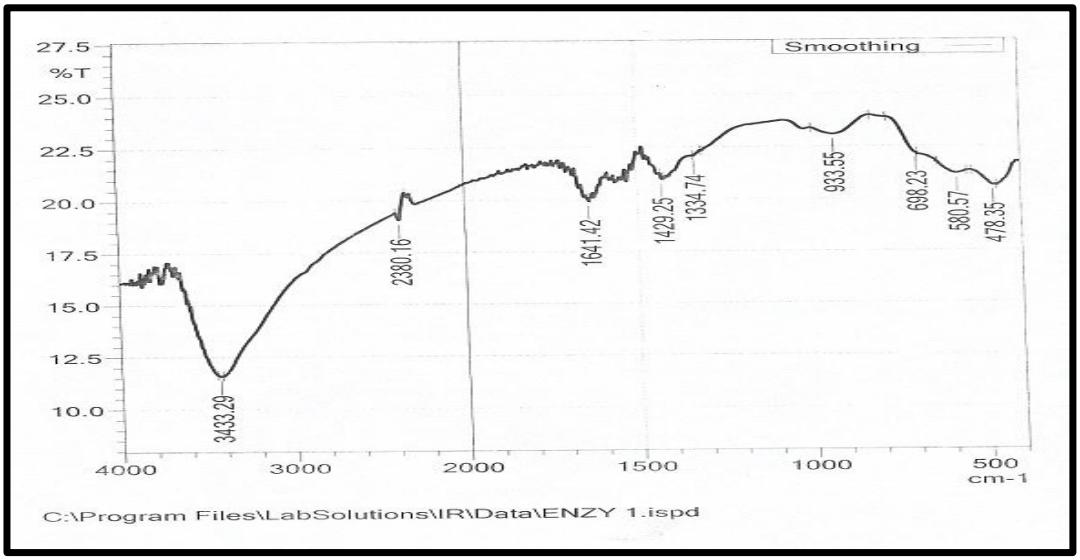


Fig 1: FTIR spectrum of C-$Fe_3O_4$

Fig. 1 displays the FTIR spectrum of the iron nanoscale supported by chitosan before adsorption. The spectrum shows a distinctive band at 3433.29 $cm^{-1}$, which indicates the existence of a –OH on the adsorbent surface. The vibration band about 1641 $cm^{-1}$ shows that C=O is present. The range of 698–478 $cm^{-1}$ is attributed to iron nanoparticles found.

*3.3 Determination of Maximum Wavelength and Standard Calibration curve for Rhodamine B.*

The different concentrations of Rhodamine B ranging from 100-1000 ppm were prepared (Fig. 2) and the standard calibration curve was determined at 554 nm using UV-VIS Spectrophotometer.

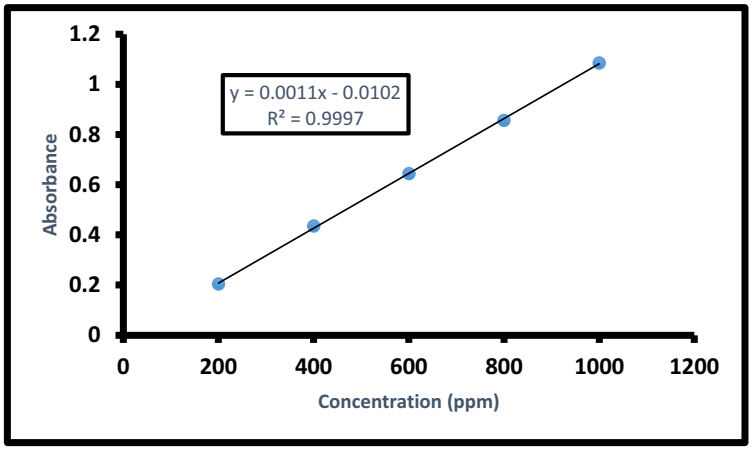


Fig 2: Standard calibration curve for Rhodanine B

### *3.4. Optimization and Effect of Operational Parameters*

#### *3.4.1 Influence of Initial RhB Concentration.*

In order to reduce the resistance caused by mass transfer between the RhB and solid phase, concentration is a crucial factor [23]. This investigation (Fig. 3) examined the impact of varying the initial concentration on adsorption over a 90-minute period at 25 $^{o}$C and 0.1 g of adsorbent dosage. Adsorption of Rhodamine B was performed at the maximum wavelength of 554 nm. The elimination effectiveness of RhB at various starting concentrations is displayed in Fig. 3. Results showed that there was a considerable decrease in amount of Rhodamine B dye adsorbed as the initial concentration increased. Hence optimum removal capacity of the adsorbent is at lower concentrations. This could be attributed to the fact that lower concentrations provide more adsorption sites on the surface of he adsorbent.

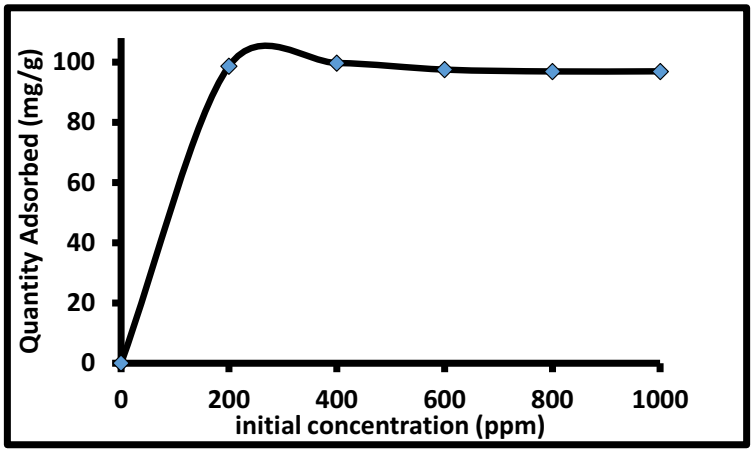


Fig 3: Effect of initial concentration (C-$Fe_3O_4$, w=0.1 g, Temp 25 $^{o}$C, for 1hr 30 mins at 120 rpm)

#### *3.4.2 Influence of Contact Time on RhB Adsortion.*

In all transfer phenomena, including adsorption, contact time is also a crucial component. The quantity of zerovalent iron required for Rhodamine B adsorption was optimized at various initial concentrations (200–1000 ppm) between 10 min and 120 min. As shown in Fig. 4, regarding C-$Fe_3O_4$, the reaction rate began quickly at 10 minutes and reached equilibrium at 30 minutes. Followed by a steady state approximation which took hold until a quasi-equilibrium state was reached [29]. This could also be attributed to the presence of more active adsorption sites at the initial 10 minutes.

For C-$Fe_3O_4$, the removal efficiency was quick during the first phase of the contact duration. A rise in quantity of accessible sites for adsorption led to an improvement in the uptake efficiency for C-$Fe_3O_4$. Fig. 4 demonstrated that the percentage adsorption maintained a steady adsorption equilibrium at these various concentrations.

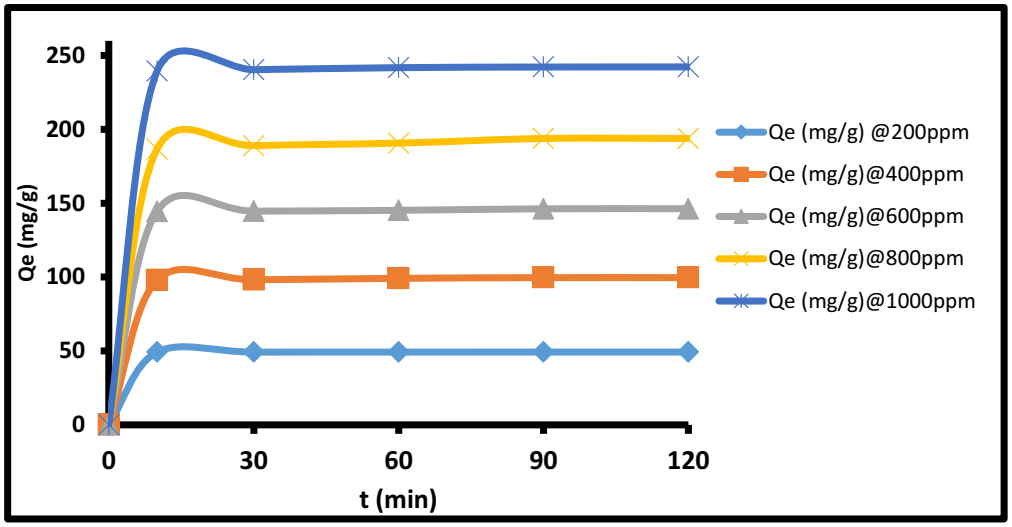


Fig 4: Influence of contact time (C-$Fe_3O_4$, w=0.1 g, Temp 25 $^oC$, for 1 hr 30 mins at 120rpm

## 5. Conclusion and Recommendation

This study reported the preparation of chitosan supported magnetite nanocomposites (C-$Fe_3O_4$). The physicochemical characterization and influence of the time of contact and initial RhB concentration and on the sorption of the dye on as-synthesized chitosan supported magnetite nanocomposites. The physicochemical and spectroscopic characterization revealed the potential of magnetite nanocomposites (C-$Fe_3O_4$) to adsorb Rhodamine B dye. Functional group of C-$Fe_3O_4$ determined by FTIR revealed characteristics peaks that confirmed the successful formation by incorporation of chitosan and magnetite nanoparticles. The adsorption studies further revealed the efficiency of the prepared nanocomposite to sequester Rhodamine B dye from water. We therefore recommend that further studies be carried out on the application of magnetite nanocomposites for other environmental pollutants.

## Acknowledgements

The authors acknowledge and appreciate the Proprietor of Landmark University for creating an empowering atmosphere for this research.

## References

[1] J. O. Ojediran, A. O. Dada, S. O. Aniyi, R. O. David, and A. D. Adewumi, “Mechanism and isotherm modeling of effective adsorption of malachite green as endocrine disruptive dye using Acid Functionalized Maize Cob (AFMC),” *Sci. Rep.*, vol. 11, no. 1, pp. 1–15, 2021, doi: 10.1038/s41598-021-00993-1.

[2] P. S. Steplin *et al.*, “Photocatalytic Degradation of Rhodamine B Using Zinc Oxide Activated Charcoal Polyaniline Nanocomposite and Its Survival Assessment Using Aquatic Animal Model,” *Sustain. Chem. Eng.*, vol. 6, pp. 258–267, 2018, doi: 10.1021/acssuschemeng.7b02335.

[3] H. Y. Gan, L.-E. Leow, and S.-T. Ong, "Utilization of corn cob and TiO2 photocatalyst thin films for dyes removal," *Acta Chim. Slov.*, vol. 64, no. 1, pp. 144–158, 2017, doi: 10.17344/acsi.2016.2983.

[4] A. O. Dada *et al.*, "Sustainable and low-cost Ocimum gratissimum for biosorption of indigo carmine dye: kinetics, isotherm, and thermodynamic studies," *Int. J. Phytoremediation*, vol. 22, no. 14, pp. 1524–1537, 2020, doi: 10.1080/15226514.2020.1785389.

[5] E. K. Guechi and O. Hamdaoui, "Sorption of malachite green from aqueous solution by potato peel: Kinetics and equilibrium modeling using non-linear analysis method," *Arab. J. Chem.*, vol. 9, pp. S416–S424, 2016, doi: 10.1016/j.arabjc.2011.05.011.

[6] A. O. Dada *et al.*, "Sustainable and low-cost Ocimum gratissimum for biosorption of indigo carmine dye: kinetics, isotherm, and thermodynamic studies," *Int. J. Phytoremediation*, vol. 0, no. 0, pp. 1–14, 2020, doi: 10.1080/15226514.2020.1785389.

[7] H. T. Hii, "Adsorption Isotherm And Kinetic Models For Removal Of Methyl Orange And Remazol Brilliant Blue R By Coconut Shell Activated Carbon," *Trop. Aquat. Soil Pollut.*, vol. 1, no. 1, pp. 1–10, 2021, doi: 10.53623/tasp.v1i1.4.

[8] O. S. Bello, M. Abiola, B. Adenike, and I. Christianah, "Ibuprofen removal using coconut husk activated Biomass," *Chem. Data Collect.*, vol. 29, p. 100533, 2020, doi: 10.1016/j.cdc.2020.100533.

[9] A. Karamipour, P. Khadiv Parsi, P. Zahedi, and S. M. A. Moosavian, "Using Fe3O4-coated nanofibers based on cellulose acetate/chitosan for adsorption of Cr(VI), Ni(II) and phenol from aqueous solutions," *Int. J. Biol. Macromol.*, vol. 154, no. Vi, pp. 1132–1139, 2020, doi: 10.1016/j.ijbiomac.2019.11.058.

[10] I. O. Saheed, W. Da Oh, and F. B. M. Suah, "Chitosan modifications for adsorption of pollutants – A review," *J. Hazard. Mater.*, vol. 408, p. 124889, 2021, doi: 10.1016/j.jhazmat.2020.124889.

[11] D. A. Oluwasogo, S. Varangane, Y. T. Prabhu, B. M. Abraham, V. Perupogu, and U. Pal, "Biosynthetic modulation of carbon-doped ZnO for rapid photocatalytic endocrine disruptive remediation and hydrogen evolution," *J. Clean. Prod.*, p. 136393, 2023, doi: https://doi.org/10.1016/j.jclepro.2023.136393.

[12] S. Bayda, M. Adeel, T. Tuccinardi, M. Cordani, and F. Rizzolio, "The history of nanoscience and nanotechnology: From chemical-physical applications to nanomedicine," *Molecules*, vol. 25, no. 1, pp. 1–15, 2020, doi: 10.3390/molecules25010112.

[13] S. Malik, K. Muhammad, and Y. Waheed, "Nanotechnology: A Revolution in Modern Industry," *Molecules*, vol. 28, no. 2, p. 661, 2023, doi: 10.3390/molecules28020661.

[14] H. Mohammadi, E. Nekobahr, J. Akhtari, M. Saeedi, J. Akbari, and F. Fathi, "Synthesis and characterization of magnetite nanoparticles by co-precipitation method coated with biocompatible compounds and evaluation of in-vitro cytotoxicity," *Toxicol. Reports*, vol. 8, pp. 331–336, 2021, doi: 10.1016/j.toxrep.2021.01.012.

[15] Z. I. Takai, M. K. Mustafa, S. Asman, and K. A. Sekak, "Preparation and characterization of Magnetite (Fe3O4) nanoparticles by Sol-Gel Method," *Int. J. Nanoelectron. Mater.*, vol. 12, no. 1, pp. 37–46, 2019.

[16] M. Imran *et al.*, "Effect of biochar modified with magnetite nanoparticles and HNO3 for efficient removal of Cr(VI) from contaminated water: A batch and column scale study," *Environ. Pollut.*, vol. 261, p. 114231, 2020, doi: 10.1016/j.envpol.2020.114231.

[17] S. G. Muntean, M. A. Nistor, E. Muntean, A. Todea, R. Ianoş, and C. Păcurariu, "Removal of Colored Organic Pollutants from Wastewaters by Magnetite/Carbon Nanocomposites: Single and Binary Systems," *J. Chem.*, vol. 2018, 2018, doi: 10.1155/2018/6249821.

[18] A. O. Dada, A. A. Inyinbor, B. E. Tokula, O. S. Bello, and U. Pal, "Preparation and characterization of rice husk activated carbon-supported zinc oxide nanocomposite (RHAC-ZnO-NC)," *Heliyon*, vol. 8, no. July, p. e10167, 2022, doi: 10.1016/j.heliyon.2022.e10167.

[19] A. O. Dada, A. A. Inyinbor, O. S. Bello, and B. E. Tokula, "Novel plantain peel activated carbon – supported zinc oxide nanocomposites (PPAC-ZnO- NC) for adsorption of chloroquine synthetic pharmaceutical used for COVID - 19 treatment," *Biomass Convers. Biorefinery*, no. 0123456789, 2021, doi: 10.1007/s13399-021-01828-9.

[20] B. E. Tokula *et al.*, "Preparation, Physicochemical and Spectroscopic Characterization of Low-Cost Acid Functionalised Rice Husk Activated Carbon (AF-RHAC)," *2023 Int. Conf. Sci. Eng. Bus. Sustain. Dev. Goals Omu-Aran, Niger.*, pp. 1-6, 2023, doi: doi: 10.1109/SEB-SDG57117.2023.10124611.

[21] K. S. Obayomi, S. Y. Lau, A. Zahir, A. O. Dada, and M. M. Rahman, "Removing Methylene Blue from Water: A study of sorption effectiveness onto nanoparticles-doped activated carbon," *Chemosphere*, vol. 313, no. 137533, 2023, doi: https://doi.org/10.1016/j.chemosphere.2022.137533.

[22] A. A. Inyinbor, F. A. Adekola, and G. A. Olatunji, "Kinetics , isotherms and thermodynamic modeling of liquid phase adsorption of Rhodamine B dye onto Raphia hookerie fruit epicarp," *Water Resour. Ind.*, vol. 15, pp. 14–27, 2016, doi: 10.1016/j.wri.2016.06.001.

[23] B. E. Tokula, A. O. Dada, A. A. Inyinbor, K. S. Obayomi, O. S. Bello, and U. Pal, "Agro-waste based adsorbents as sustainable materials for effective adsorption of Bisphenol A from the environment : A review," *J. Clean. Prod.*, vol. 388, p. 135819, 2023, doi: 10.1016/j.jclepro.2022.135819.

[24] O. S. Agboola, S. B. Akanji, and O. S. Bello, "Functionalized Banana Stalk for Lumefantrine Drug Removal," *Phys. Chem. Res.*, vol. 9, no. 3, pp. 483–507, 2021, doi: 10.22036/pcr.2021.261506.1865.

[25] F. Nworie, E. Oroke, I. Ikelle, and J. Nworu, "Equilibrium and Kinetic Studies for The Adsorptive Removal of Lead (II) Ions from Aqueous Solution Using Activated Plantain Peel Biochar," *Acta Chem. Malaysia*, vol. 4, no. 1, pp. 9–16, 2020, doi: 10.2478/acmy-2020-0002.

[26] F. A. Dawodu, B. M. Akpan, and K. G. Akpomie, "Sequestered capture and desorption of hexavalent chromium from solution and textile wastewater onto low cost Heinsia crinita seed coat biomass," *Appl. Water Sci.*, vol. 10, no. 1, 2020, doi: 10.1007/s13201-019-1114-6.

[27] F. Gündüz and B. Bayrak, "Biosorption of malachite green from an aqueous solution

using pomegranate peel: Equilibrium modelling, kinetic and thermodynamic studies," *J. Mol. Liq.*, vol. 243, pp. 790–798, 2017, doi: 10.1016/j.molliq.2017.08.095.

[28] M. R. Abukhadra, B. M. Bakry, A. Adlii, S. M. Yakout, and M. A. El-Zaidy, "Facile conversion of kaolinite into clay nanotubes (KNTs) of enhanced adsorption properties for toxic heavy metals (Zn2+, Cd2+, Pb2+, and Cr6+) from water," *J. Hazard. Mater.*, vol. 374, no. January, pp. 296–308, 2019, doi: 10.1016/j.jhazmat.2019.04.047.

[29] O. S. Bello, O. C. Alao, T. C. Alagbada, O. S. Agboola, O. T. Omotoba, and O. R. Abikoye, "A renewable, sustainable and low-cost adsorbent for ibuprofen removal," *Water Sci. Technol.*, vol. 83, no. 1, pp. 111–122, 2021, doi: 10.2166/wst.2020.551.